




Research Article

Application of Attapulgitic Clay-Based Fe-Zeolite 5A in UV-Assisted Catalytic Ozonation for the Removal of Ciprofloxacin

Amir Ikhlaq ¹, Rahat Javaid ², Asia Akram,³ Umair Yaqub Qazi ⁴, Javeria Erfan,¹ Metwally Madkour,⁵ Mohamed Elnaiem M. Abdelbagi,⁴ Sami M. Ibn Shamsah,⁶ and Fei Qi⁷

¹Institute of Environmental Engineering and Research, University of Engineering and Technology, Lahore, Pakistan

²Renewable Energy Research Center, Fukushima Renewable Energy Institute, National Institute of Advanced Industrial Science and Technology, AIST, 2-2-9 Machiikedai, Koriyama, Fukushima 963-0298, Japan

³University of Management and Technology, Johar Town, Lahore, Pakistan

⁴Department of Chemistry, College of Science, University of Hafr Al Batin, P.O. Box 1803, Hafr Al Batin 39524, Saudi Arabia

⁵Chemistry Department, Faculty of Science, Kuwait University, P.O. Box 5969, Safat 13060, Kuwait

⁶Department of Mechanical Engineering, College of Engineering, University of Hafr Al Batin, P.O. Box 1803, Hafr Al Batin 31991, Saudi Arabia

⁷Beijing Forestry University, No. 35 Qinghua East Road, Haidian District, Beijing 100083, China

Correspondence should be addressed to Amir Ikhlaq; amirikhlaq@uet.edu.pk and Umair Yaqub Qazi; umairqazi@uhb.edu.sa

Received 19 July 2021; Accepted 22 April 2022; Published 19 May 2022

Academic Editor: Hassan Arida

Copyright © 2022 Amir Ikhlaq et al. This is an open access article distributed under the Creative Commons Attribution License, which permits unrestricted use, distribution, and reproduction in any medium, provided the original work is properly cited.

For the first time, Fe-zeolite 5A (Fe-Z5A) efficacy in the UV-assisted ozonation process to remove ciprofloxacin (CF) in wastewater is investigated. FTIR, SEM, EDX, BET, and the mass transfer process for point of zero charge are used to characterize the catalyst. Furthermore, the synergic process (UV/O₃/Fe-Z5A) is compared with O₃, O₃/UV, and Fe-Z5A/O₃ processes. The influence of catalyst dose, hydroxyl radical scavenger, and off-gas ozone released is discussed. The removal efficiency of CF in wastewater (for the synergic process) is compared with a single ozonation process. The results indicate that the synergic process was more efficient than others, with about 73% CF being removed (in 60 minutes) in the synergic process. The results also show that synergic processes produce less off-gas ozone than other processes, suggesting more ozone consumption in the synergic process, and confirmed by the radical scavenger effect and hydrogen peroxide decomposition studies. The Fe-Z5A was found to operate through a hydroxyl mechanism in which Fe worked as an active site that promotes the formation of hydroxyl radicals. Finally, the synergic process was more efficient than the ozonation process in the wastewater matrix. Hence, Fe-Z5A/O₃/UV pathway is highly efficient for the degradation of pharmaceuticals in wastewater.

1. Introduction

Photocatalytic ozonation processes are among the best choices for advanced oxidation processes (AOPs) used in wastewater treatment [1–6]. A variety of materials are used as catalysts in these processes, such as activated carbons [7, 8], metal oxides [9–12], and organic-based photocatalysts [13–15]. Due to their stability and selectivity, zeolites were found to be highly significant for practical applications [16–22]. They have already been practically implied as a catalyst, ion-exchanger, and adsorbent in dif-

ferent areas [23–26]. Their unique properties such as silica to alumina ratios, shapes, surface area, and Lewis and Bronsted acid sites make them quite useful option in wastewater treatment [23–25, 27]. Zeolites of different types were successfully studied in the past as catalysts in catalytic ozonation processes, such as ZSM-5, Y-zeolites, MCM-41, zeolite 4A, and natural zeolites [23–25, 27–30].

In recent few years, metal-loaded zeolites were extensively implied as a catalyst in ozone-assisted processes and were found to be highly efficient [31, 32]. Since each type of zeolite may have unique properties and shapes compared

to others, it is indeed important to investigate the ozone-assisted processes in the presence of various types of zeolites. This study is the continuation of the author's previous studies to investigate the applicability and behavior of multiple types and forms of zeolites in ozone-assisted catalytic processes [28, 33]. In this investigation, a comparative study was conducted between UV-assisted and catalytic ozonation processes using iron-coated zeolite 5A (Z5A) as a potential catalyst. To the best of the author's knowledge, this is the first report in which zeolite 5A was tested as a catalyst in the UV-assisted catalytic ozonation process. González-Labrada et al. [34] recently studied the degradation of ciprofloxacin on Fe-MFI zeolites and found significantly higher CF removal than ozonation alone, while the current investigation is based on the UV-irradiated catalytic ozonation process with iron-loaded zeolite and compared with simple catalytic ozonation process. It is significant to mention here that in hydroxyl radical-based catalytic ozonation processes, the hydroxyl radicals in aqueous solutions may combine to form hydrogen peroxide, which may have a negative effect on overall removal efficiency [35]. Therefore, in the current investigation, UV-assisted catalytic ozonation on Fe-Z5A was considered to further decompose hydrogen peroxide (through direct UV irradiation, ozone UV interactions, and Fenton-like decomposition on catalyst surface). Therefore, this study may further help to understand the applicability of a different type of zeolites in natural conditions using a UV-assisted process.

In the current investigation, the antibiotic ciprofloxacin (CF) was selected as the target pollutant. The occurrence of antibiotics was identified even in drinking water across the world [36, 37]. The conventional biological wastewater treatment methods failed to degrade antibiotics and other pharmaceuticals completely, and they were found in their effluents [38]. The continuous exposure of our environment to antibiotics is not only hazardous to human and aquatic organisms but it may result in the evolution of antibiotic-resistant microorganisms in the future [39–42]. These microbes may pose a severe threat to humanity; therefore, it is essential to find novel methods that may be applied in combination with biological processes to eliminate threats to our future generations.

In the current investigation, UV-assisted catalytic ozonation process using iron-loaded zeolite 5A was studied to remove CF. The 5A type of molecular sieves is aluminosilicate Linde type A (LTA) form of zeolites that contain calcium instead of sodium ion having diameter of 5 Å. These types of zeolites are well known for their ability to adsorb pollutants. Therefore, in current investigation, 5A type zeolites loaded with iron were used as catalyst in the ozonation process. Moreover, the catalyst dose effect, hydroxyl radical scavenger (t-butanol), and removal of CF in denoised and wastewater were investigated.

2. Experimental

2.1. Materials and Reagents. The zeolite 5A, ciprofloxacin, and t-butanol (used for hydroxyl radical scavenger effect)

were obtained from Sigma-Aldrich (UK). All chemicals were of analytical grade and used without further purification.

2.2. Catalyst Preparation. The Z5A obtained from Sigma-Aldrich (UK) was washed several times with ultrapure deionized water to remove impurities (if any) from Z5A. The iron-loaded Z5A was prepared by using the incipient impregnation method [43–45]. In this method, a weighed amount (6 g) of ferric nitrate nonahydrate ($\text{Fe}(\text{NO}_3)_3 \cdot 9\text{H}_2\text{O}$) was taken in a beaker that contains 20 mL ultrapure deionized water. Then, Z5A (10 g) was placed into the beaker containing iron salt and was continuously stirred at 120 rpm at 100°C till the water evaporated. Then, Fe-Z5A was calcined at 500°C during 4 hrs [43–45]. The Fe-Z5A was dipped into (0.1 M) HNO_3 for 24 hours to remove any unattached iron. Then, it was filtered and washed several times with ultrapure deionized water till the pH of washout water remains constant. Finally, the catalyst was dried in an oven at 103°C overnight [43–45].

2.3. Experimental Procedure. Experiments involving photocatalytic ozonation, catalytic ozonation, and single ozonation were carried out in a semicontinuous reactor (Figure 1). The reactor was installed with UV-light (UV rays (20 W), a wavelength of 254 nm obtained from UV rod (Sylvania Pvt Ltd., Germany). In this study, 2.5 L working solution of ciprofloxacin (initial concentration = 50 ppm) was placed in the reactor. The ozone was introduced (Sky Zone, DA12025B12L, Karachi, Pakistan) continuously into the reactor for 60 minutes. Samples were collected after fixed time intervals and were then quenched with Na_2CO_3 (0.025 M) to remove residual aqueous ozone [33]. Finally, samples were analyzed at 284 nm on HPLC (Hitachi Elite LaChrom L-2130) equipped with C18 column (4.6×250 mm, Poroshell 120). All the samples were also scanned on a UV-Vis spectrophotometer (PerkinElmer Lambda 35 double beam) between 200 nm and 700 nm to observe any byproducts formed. The removal efficiencies of CF were determined by using the following equation.

$$\text{Ciprofloxacin removal (\%)} = \frac{A_o - A_t}{A_o} \times 100, \quad (1)$$

where A_t is the peak area time t , and A_o is the peak area at $t = 0$.

2.4. Analytical Procedures

2.4.1. Ozone Dose. The ozone dose was determined by using the iodometric method described elsewhere [46]. Such ozone was bubbled into two sets of flasks (Figure 1) containing 2% KI solution (100 mL). After the entire process, 5 mL H_2SO_4 (2N) was added to each flask to liberate iodine. Then, the solution was titrated against 0.005 N $\text{Na}_2\text{S}_2\text{O}_3$ using a starch indicator [27] [46]. Ozone dose was calculated using the following formula:

$$\text{Ozone dose} \left(\frac{\text{mg}}{\text{min}} \right) = \frac{\text{Volume of titrant} * \text{normality of titrant} * 24}{\text{Time}}. \quad (2)$$

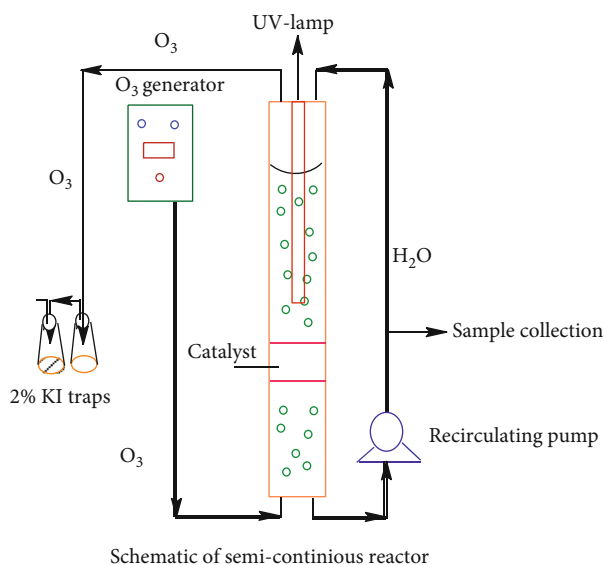


FIGURE 1: Schematic of semicontinuous reactor for the treatment of ciprofloxacin by the catalytic ozonation process.

2.4.2. Analysis of Ciprofloxacin. Ciprofloxacin concentration was quantified by determining the peak areas before and after treatment using the HPLC system (Hitachi Elite LaChrom L-2130) containing C18 column (4.6 × 250 mm, Poroshell 120). The method was developed before analysis, and the mobile phase composition was 50:50 acetonitrile-phosphate buffer (0.2 M KH_2PO_4 and 0.2 M NaOH). The samples were analyzed by injecting a 10 μL solution at a mobile phase flow rate of 1 mL/min.

2.4.3. Analysis of Hydrogen Peroxide. The amount of hydrogen peroxide was monitored by observing the resorufin fluorescence spectrum using a fluorescence spectrometer (F-4500 Japan) having 5 nm slits. Fluorescence was monitored at 587 nm (a calibration curve was drawn by reacting H_2O_2 and Amplex Red reagent [35]).

3. Results and Discussion

3.1. Catalyst Characteristics. The zeolite 5A is a calcium zeolite having the composition $\text{Ca}_{4.5} [(\text{AlO}_2)_{12}(\text{SiO}_2)_{12}] n\text{H}_2\text{O}$. The catalyst was loaded with Fe^{+3} by the impregnation method [47], and the presence of iron on the catalyst was confirmed by FTIR analysis, using PerkinElmer (USA) spectrum 400 analyzer. The results presented in Figure 2 clearly show the iron loading on Z5A. The spectra indicate that a sharp peak at about 970 cm^{-1} reflects stretching vibrations of Si-O and Al-OH [45]. A comparative study shows that a new peak at about $1,442\text{ cm}^{-1}$ is due to iron loading and corresponds to Fe-OH stretching vibrations [45]. The Fe-Z5A surface morphology (Figure 3) and elemental analysis were investigated by SEM-EDX using Tescan, (UK), Vega LMU. The iron was found to be 5%. The SEM image (Figure 2) shows that the surface of the catalyst was smooth and porous. The surface area and pore size were quantified by the BET method. The nitrogen adsorption at 77 K was

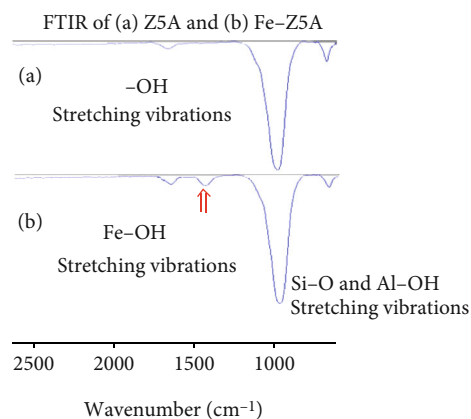


FIGURE 2: FTIR spectra of Z5A and Fe-Z5A.

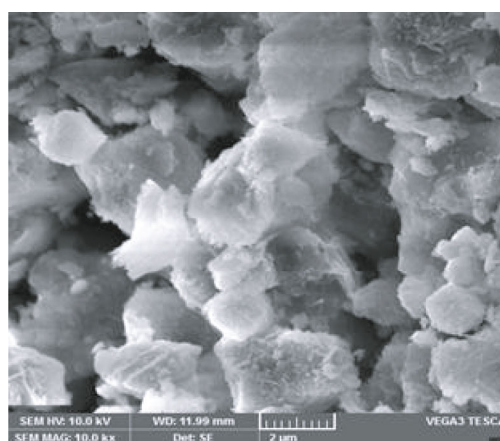


FIGURE 3: SEM image of Fe-Z5A.

determined by using adsorption isotherms (Figure 4). The Kelvin equation and BJH method were adopted for the determination of porosities [28]. The surface area of Fe-Z5A was $93.25\text{ m}^2/\text{g}$, and the pore size was 5 \AA . The mass titration method was used to determine the point of zero charge of Fe-Z5A [48] and was found to be 6.6.

3.2. Comparison of Studied AOPs. The results presented in Figure 5 indicate the comparison between various advanced oxidation processes under similar conditions. The highest removal efficiency was observed for the synergic ($\text{O}_3/\text{Fe-Z5A}/\text{UV}$) process. For example, the removal efficiencies (in 60 minutes) were 73.4%, 65.6%, 57.1%, and 49.3% for $\text{O}_3/\text{Fe-Z5A}/\text{UV}$, $\text{O}_3/\text{Fe-Z5A}$, O_3/UV , and O_3 , respectively (Figure 4). The synergic process (catalytic ozonation with UV irradiation) involves various reactions leading to the production of hydroxyl radicals (equations (3)–(7)). These reactions involves the interaction of ozone with the active sites of catalyst (Fe) leading to the production of hydroxyl radicals (equations (3)–(7)) [35, 49, 50]. In addition, the catalyst may be activated by UV irradiation resulting in the formation of hydroxyl radicals (equation (8)) [51]. The interactions of molecular ozone with UV radiations may also facilitate the production of hydroxyl radicals (equations (9))

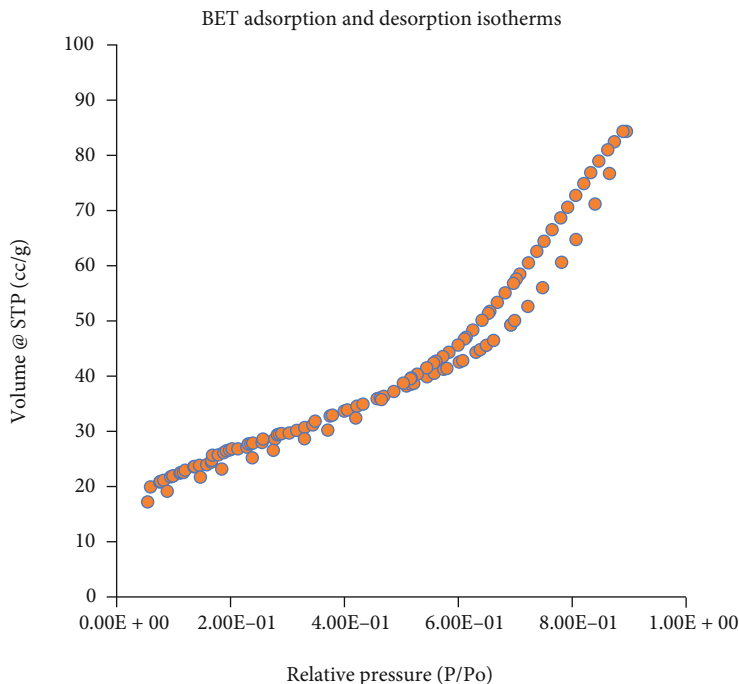
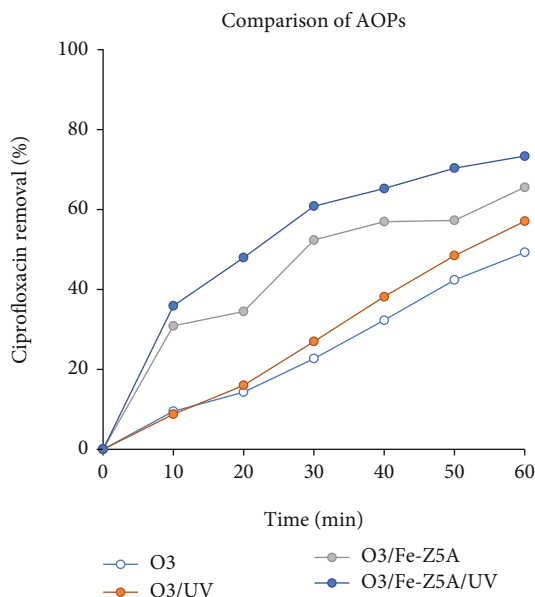
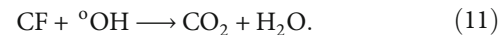
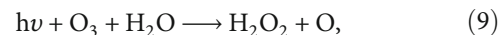
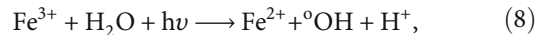
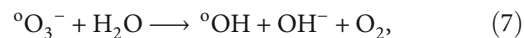
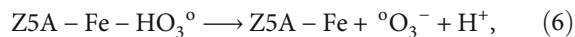
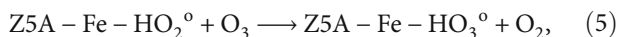
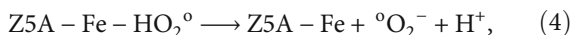
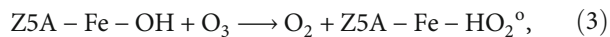


FIGURE 4: BET isotherm of Fe-zeolite A.

FIGURE 5: Comparison of AOPs for the removal of ciprofloxacin ($C_{o(\text{cipro})} = 50 \text{ mg/L}$; $\text{pH} = 6.5 \pm 0.2$; $\text{O}_3 = 0.9 \text{ mg/L}$; volume = 2.5 L; catalyst dose = 25 g; $T = 60 \text{ min}$).

and (10)) [52] that reacts with CP leading to its degradation (equation (11)).



Additionally, the significantly higher removal efficiency of the O_3/UV process compared to O_3 alone (Figure 5) suggested that UV-rays were involved in the decomposition of ozone, resulting in the production of active oxygen species, and enhance the removal [52].

The adsorption of pollutants on the catalyst surface may also play an important role in the overall removal efficiency of pollutants in water. Therefore, the charge on the pollutant and catalyst may be important in such studies. The point of zero charge of catalyst and pKa values of pollutants may help to identify charges on them while comparing with the initial pH of water [50, 53, 54]. Therefore, in catalytic processes, the point of zero charge of catalyst and pKa values of CF plays an important role [55]. Since the pKa_1 (6.0) of CF is near the point of zero charge ($\text{pH} = \text{pH}_{\text{pzc}}$) of Fe-Z5A, pKa_2 (8.8) is more than the pH of the CP solution (CP solution: $\text{pH} = 6.5 \pm 0.2$). Thus, at the analyzed pH, the CF may acquire a positive charge (pKa_2 is more than solution pH, while the zeolite surface may have a slight negative charge (as pH_{pzc} of zeolite is slightly above CP solution pH)); this further aids in the adsorption of CF on the catalyst surface

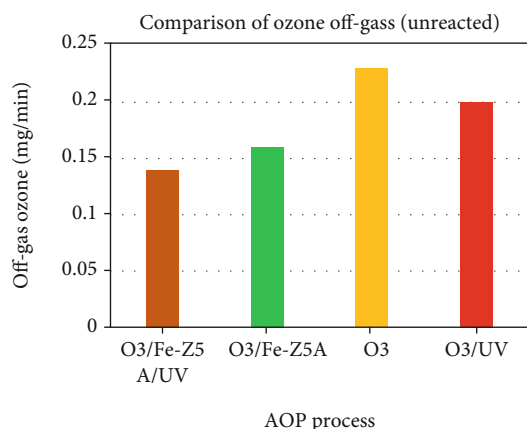


FIGURE 6: Comparison of AOPs for off-gas measured from KI traps during the removal of ciprofloxacin ($C_{o(\text{cipro})} = 50 \text{ mg/L}$; $\text{pH} = 6.5 \pm 0.2$; $\text{O}_3 = 0.9 \text{ mg/L}$; volume = 2.5 L; catalyst dose = 25 g; $T = 60 \text{ min}$).

and has a positive impact on the removal performance as compared to processes without catalyst [50, 53, 54].

It is worth mentioning that gaseous ozone (unreacted) released from the reactor was measured (Figure 6). It was also observed that the synergic process produced the least amount of ozone (mg/min). For example, 0.14 mg/min, 0.16 mg/min, 0.2 mg/min, and 0.23 mg/min were quantified for O₃/Fe-Z5A/UV, O₃/Fe-Z5A, O₃UV, and O₃ processes, respectively (Figure 6). The results exhibit an important correlation between the CF removed and off-gas ozone released in various processes. The off-gas ozone released in above-mentioned processes was in the opposite order to the removal efficiency of CF in the various processes (Figures 5 and 6). The synergic process was found to have the least off-gas ozone release. It is hypothesized that more ozone decomposition may result in the production of active oxygen species compared to others in the synergic process.

3.3. Catalyst (Fe-Z5A) Dose Effect. It is essential to investigate the role of the proposed catalyst in UV and O₃; therefore, the catalyst dose effect is studied. The results presented in Figure 7 indicate that with an increase in catalyst dose, the removal efficiency of CF improved for both UV/O₃/Fe-Z5A and O₃/Fe-Z5A processes. Hence, it is suggested that a higher catalyst dose increases the number of active sites, leading to more decomposition of aqueous ozone and the generation of hydroxyl radicals.

3.4. Ciprofloxacin Removal in Municipal Wastewater. In this study, the CF was spiked in municipal wastewater samples to investigate the removal efficiency of the synergic process in a real wastewater matrix. In most of the previous findings, aqueous solutions of pharmaceuticals were prepared to investigate the processes. However, it is indeed essential to test a catalytic process in real conditions since the wastewater matrix is more complex and contains inhibitors such as turbidity, radical scavengers, bacteria etc.

The results presented in Figure 8 show that the removal efficiency of the synergic process was decreased significantly

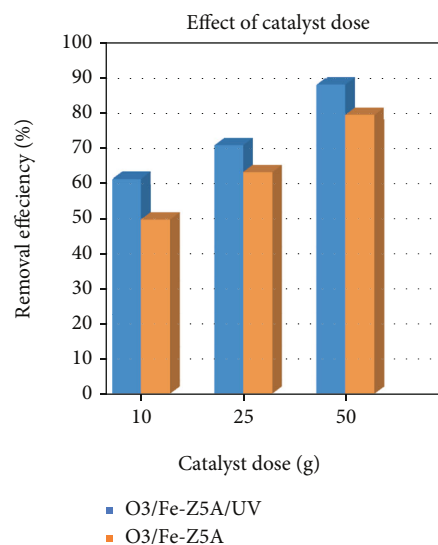


FIGURE 7: Catalyst dose effect on ciprofloxacin removal ($C_{o(\text{cipro})} = 50 \text{ mg/L}$; $\text{pH} = 6.5 \pm 0.2$; $\text{O}_3 = 0.9 \text{ mg/L}$; volume = 2.5 L; catalyst dose = 10 g, 25 g, and 50 g; $T = 60 \text{ min}$).

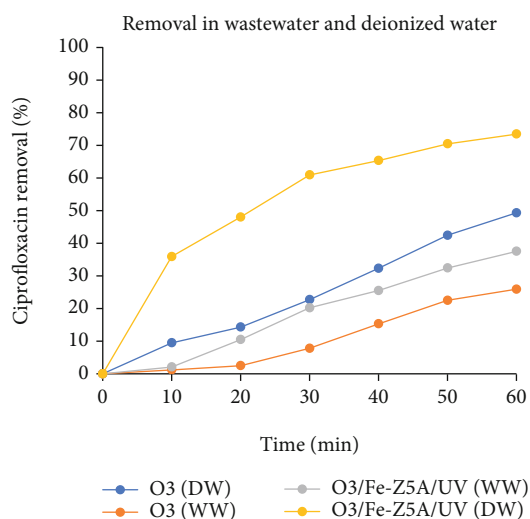


FIGURE 8: Comparison of ciprofloxacin removal in municipal wastewater and deionized water using O₃ and UV/O₃/FeZ5A ($C_{o(\text{cipro})} = 50 \text{ mg/L}$; COD = 104 mg/L; $\text{pH}_{\text{DW}} = 6.5 \pm 0.2$; $\text{pH}_{\text{WW}} = 7.2 \pm 0.2$; $\text{O}_3 = 0.9 \text{ mg/L}$; volume = 2.5 L; catalyst dose = 25 g; $T = 60 \text{ min}$).

in wastewater. This may be due to the presence of inhibitors in wastewater [56]. Furthermore, the COD in wastewater due to organic pollutants may also compete with the removal of CF. Interestingly, when the results were compared with single ozonation, it was observed that the efficiency of CF removal was significantly higher in catalytic ozonation process as compared with ozonation alone in both the deionized water and wastewater (Figure 8). For example, the removal efficiency (in 60 minutes) of CF was 49.3%, 37.5%, and 25.9% for synergic process in wastewater, single ozonation in wastewater, and single ozonation in deionized

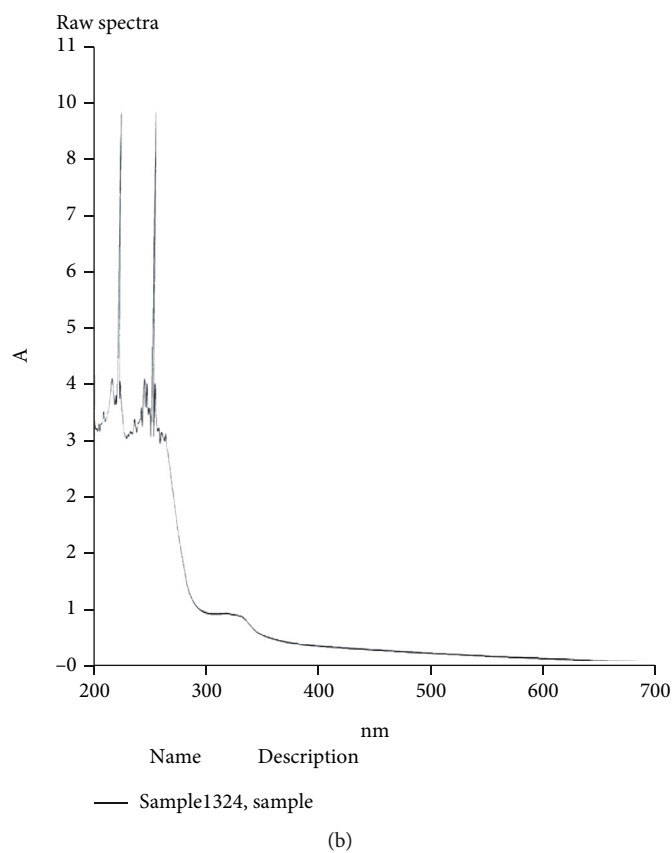
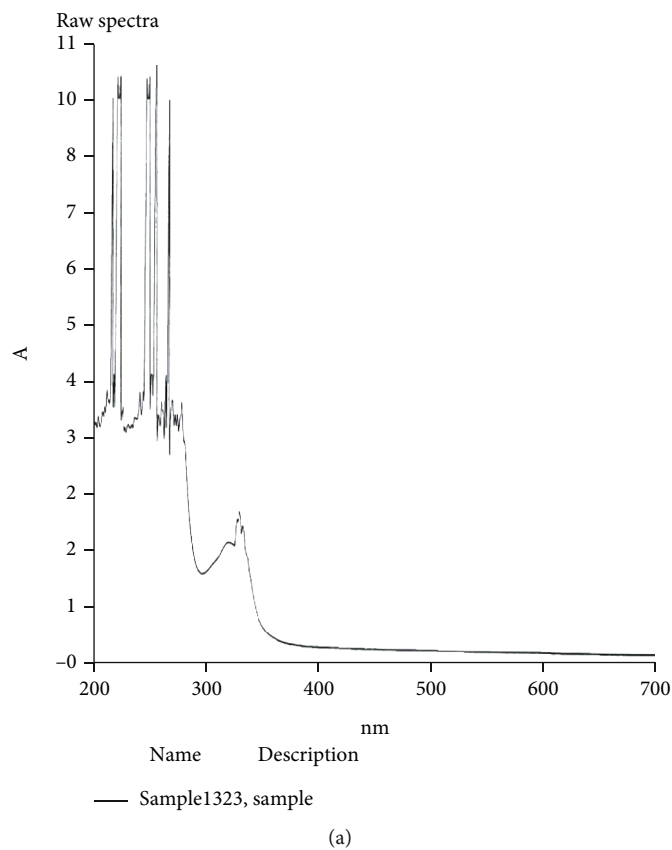


FIGURE 9: Spectrophotometer analysis of wastewater before (a) and after treatment (b) with the UV/Fe-Z5A/O₃ process (spiked $C_{o(cipro)}$ = 50 mg/L; COD = 104 mg/L; pH = 7.2 ± 0.2; O₃ = 0.9 mg/L; volume = 2.5 L; catalyst dose = 25 g; T = 60 min).

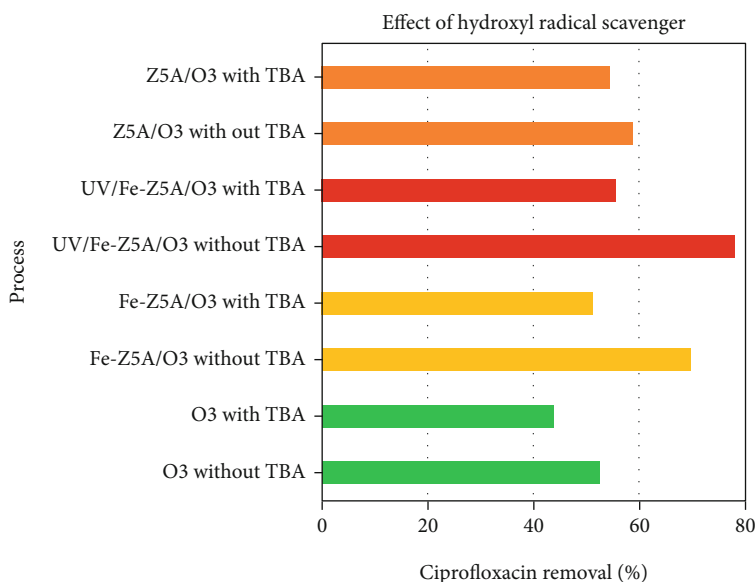


FIGURE 10: TBA effect on ciprofloxacin removal for O_3 , $O_3/Z5A$, $O_3/Fe-Z5A$, and $UV/O_3/FeZ5A$ processes ($C_{o(cipro)} = 50$ mg/L; TBA = 50 ppm; pH = 6.5 ± 0.2 ; $O_3 = 0.9$ mg/L; volume = 2.5 L; catalyst dose = 25; $T = 60$ min).

water, respectively (Figure 7). Therefore, the results suggest that the synergic process ($UV/O_3/Fe-Z5A$) is even effective in real conditions for the removal of pharmaceuticals in wastewater. The UV scan of CF spiked wastewater before and after treatment with a synergic process (Figure 9) also clearly indicates the removal of organic pollutants in the presence of the synergic process.

3.5. Mechanism of Synergic Process

3.5.1. Radical Scavenger Effect. The t-butanol, due to its high rate of reaction with hydroxyl radicals, was found to be effective in investigating the production of hydroxyl radicals in AOPs [57]. The current investigation results (Figure 10) suggested that the synergic process involves the radical-based mechanism. Moreover, in the synergic process, more decrease in removal efficiency was observed with TBA than other studied processes. This further supports our hypothesis that the synergic process is highly effective compared to others because it leads to the more decomposition of aqueous ozone, leading to hydroxyl radicals (Figure 10). Interestingly, the findings presented in Figure 10 agree with the results of off-gas ozone shown in Figure 5.

When the results were compared to single ozonation, the results indicate that in the $Z5A/O_3$ process, no significant decrease in CP efficiency was observed in the presence of TBA. This suggested that $Z5A/O_3$ removes CF through a nonradical mechanism [28, 33]. In contrast, iron-loaded zeolites follow a radical mechanism (Figure 10). Therefore, the current investigation also helps further to understand the importance of iron loading on zeolites. Since wastewater is a complex media in which various kinds of radical scavengers such as phosphates and sulfates may be present in significant amounts, it is critical to select such catalysts that may follow radical and selectively nonradical mechanisms.

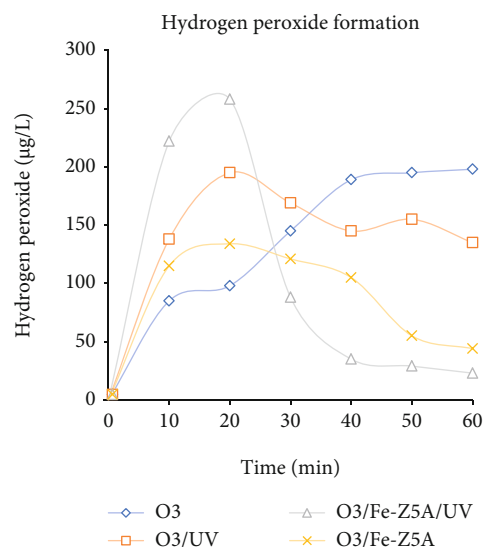


FIGURE 11: Formation of hydrogen peroxide in synergic process, catalytic ozonation, single ozonation, and ozone UV process (C_o Amplex Red = 15 mg/L; pH = 6.5 ± 0.2 ; $O_3 = 0.9$ mg/L; volume = 2.5 L; catalyst dose = 25; $T = 60$ min).

Therefore, zeolites are among the unique catalysts that may follow both mechanisms, and metal loadings on them may be significant in the generation of hydroxyl radicals [32, 49].

3.5.2. Formation of Hydrogen Peroxide. Understanding the mechanism of the synergic pathway and verifying its effectiveness, the production of H_2O_2 in various processes was investigated. The hydrogen peroxide may form either by the combination of two hydroxyl radicals in bulk or by UV irradiation of ozone in the presence of water molecules

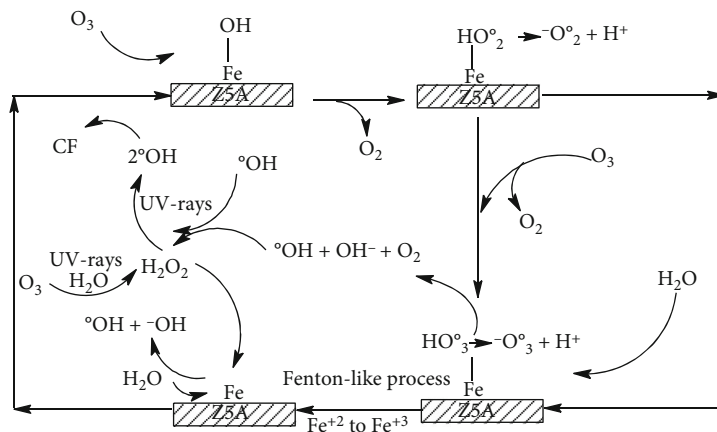
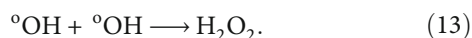


FIGURE 12: Mechanism of UV-assisted catalytic ozonation on Fe-Z5A.

[52] as shown in the following equations.



Therefore, in the catalytic ozonation process (without UV) and single ozonation process, many hydroxyl radicals may combine to form stable H_2O_2 with low reactivity with organic pollutants. Hence, in the current investigation, UV-based catalytic ozonation process may decompose the formed H_2O_2 by either a Fenton-like mechanism [58] or by UV irradiation (Figures 11 and 12).

Figure 11 indicates that H_2O_2 production was the highest in the synergic process in the first 20 minutes. On the other hand, its decomposition was also the highest in the case of the synergic process. A higher H_2O_2 was formed in the synergic process and the generation of more $^{\circ}\text{OH}$ radicals (Figure 11). Experiments further confirmed this in the presence of hydroxyl radical scavengers (Figure 9).

Interestingly, Figure 11 also shows that the formation of H_2O_2 markedly decreased after 20 minutes when the synergic process was used. This is attributed to Fenton-like decomposition on catalyst surface (Figure 11) and H_2O_2 due to UV-rays in bulk (equation (4)), leading to the generation of reactive oxygen species. Consequently, it elaborates that the effectiveness of the synergic process was due to the decomposition of H_2O_2 causing the formation of hydroxyl radicals that further leads to degradation of CF. Mechanism of UV-assisted catalytic ozonation on Fe-Z5A is fully described in Figure 12.

4. Conclusions

Based on the results, it is concluded that the synergic process (UV/ O_3 /Fe-Z5A) was the most efficient process as compared to other studied processes (O_3 , O_3 /UV, and O_3 /Fe-Z5A processes). The TBA effect suggested that the Fe-Z5A/ O_3 process degrades ciprofloxacin via hydroxyl radical-based mechanism. The synergic process was also influential in real wastewater in removing ciprofloxacin as compared with sin-

gle ozonation process. The synergic process effectively decomposes hydrogen peroxide leading to the production of fewer hydroxyl radicals than other studied processes.

Data Availability

The data used to support the findings of this study are included within the article additional information/data that will be available upon request.

Conflicts of Interest

The authors have no conflicts of interest to declare that are relevant to the content of this article.

Acknowledgments

Dr. Amir Ikhlaq and Fei Qi highly acknowledge the Pakistan Science Foundation (PSF) for their funding and support under PSF/CRP 18th Protocol (12). We highly appreciate the support of the Institute of Environmental Engineering, UET Lahore, Pakistan. In addition, the authors extend their appreciation to the Deanship of Scientific Research, University of Hafr Al Batin for financial support through the research group project No. S-0048-1443.

References

- [1] F. J. Beltrán, A. Aguinaco, J. F. García-Araya, and A. Oropesa, "Ozone and photocatalytic processes to remove the antibiotic sulfamethoxazole from water," *Water Research*, vol. 42, no. 14, pp. 3799–3808, 2008.
- [2] M. Mehrjouei, S. Müller, and D. Möller, "A review on photocatalytic ozonation used for the treatment of water and wastewater," *Chemical Engineering Journal*, vol. 263, pp. 209–219, 2015.
- [3] R. Javaid, H. Kawanami, M. Chatterjee, T. Ishizaka, A. Suzuki, and T. M. Suzuki, "Fabrication of microtubular reactors coated with thin catalytic layer (M=Pt, Pd-Cu, Pt, Rh, Au)," *Catalysis Communications*, vol. 11, no. 14, pp. 1160–1164, 2010.
- [4] R. Javaid, U. Y. Qazi, and S. I. Kawasaki, "Highly efficient decomposition of Remazol Brilliant Blue R using tubular

- reactor coated with thin layer of PdO,” *Journal of Environmental Management*, vol. 180, pp. 551–556, 2016.
- [5] R. Javaid, H. Kawanami, M. Chatterjee, T. Ishizaka, A. Suzuki, and T. M. Suzuki, “Sonogashira C-C coupling reaction in water using tubular reactors with catalytic metal inner surface,” *Chemical Engineering Journal*, vol. 167, no. 2-3, pp. 431–435, 2011.
- [6] U. Y. Qazi, Z. Shervani, and R. Javaid, “Green synthesis of silver nanoparticles by pulsed laser irradiation: effect of hydrophilicity of dispersing agents on size of particles,” *Frontiers in Nanoscience and Nanotechnology*, vol. 4, pp. 61–69, 2015.
- [7] I. Velo-Gala, J. J. López-Peñalver, M. Sánchez-Polo, and J. Rivera-Utrilla, “Activated carbon as photocatalyst of reactions in aqueous phase,” *Applied Catalysis B: Environmental*, vol. 142–143, pp. 694–704, 2013.
- [8] N. M. Mahmoodi, “Photocatalytic ozonation of dyes using multiwalled carbon nanotube,” *Journal of Molecular Catalysis A: Chemical*, vol. 366, pp. 254–260, 2013.
- [9] S. Anandan, G. J. Lee, P. K. Chen, C. Fan, and J. J. Wu, “Removal of Orange II dye in water by visible light assisted photocatalytic ozonation using Bi₂O₃ and Au/Bi₂O₃ nanorods,” *Industrial and Engineering Chemistry Research*, vol. 49, no. 20, pp. 9729–9737, 2010.
- [10] J. Xiao, Y. Xie, and H. Cao, “Organic pollutants removal in wastewater by heterogeneous photocatalytic ozonation,” *Chemosphere*, vol. 121, pp. 1–17, 2015.
- [11] A. Tabasum, M. Alghuthaymi, U. Y. Qazi et al., “Uv-accelerated photocatalytic degradation of pesticide over magnetite and cobalt ferrite decorated graphene oxide composite,” *Plants*, vol. 10, no. 1, pp. 1–18, 2020.
- [12] U. Y. Qazi, R. Javaid, N. Tahir, A. Jamil, and A. Adeel, “Design of advanced self-supported electrode by surface modification of copper foam with transition metals for efficient hydrogen evolution reaction,” *International Journal of Hydrogen Energy*, vol. 45, no. 58, pp. 33396–33406, 2020.
- [13] Y. Wang, Y. Xie, H. Sun, J. Xiao, H. Cao, and S. Wang, “Efficient catalytic ozonation over reduced graphene oxide for p-hydroxybenzoic acid (PHBA) destruction: active site and mechanism,” *ACS Applied Materials & Interfaces*, vol. 8, no. 15, pp. 9710–9720, 2016.
- [14] A. Ikhlq, R. Fatima, U. Y. Qazi et al., “Combined iron-loaded zeolites and ozone-based process for the purification of drinking water in a novel hybrid reactor: removal of faecal coliforms and arsenic,” *Catalysts*, vol. 11, no. 3, p. 373, 2021.
- [15] U. Y. Qazi, C. Z. Yuan, N. Ullah et al., “One-step growth of iron-nickel bimetallic nanoparticles on FeNi alloy foils: highly efficient advanced electrodes for the oxygen evolution reaction,” *ACS Applied Materials & Interfaces*, vol. 9, no. 34, pp. 28627–28634, 2017.
- [16] M. U. Rahman, U. Y. Qazi, T. Hussain et al., “Solar driven photocatalytic degradation potential of novel graphitic carbon nitride based nano zero-valent iron doped bismuth ferrite ternary composite,” *Optical Materials*, vol. 120, article 111408, 2021.
- [17] R. Javaid, U. Y. Qazi, A. Ikhlq, M. Zahid, and A. Alazmi, “Subcritical and supercritical water oxidation for dye decomposition,” *Journal of Environmental Management*, vol. 290, article 112605, 2021.
- [18] A. Ikhlq, F. Javed, A. Akram et al., “Treatment of leachate through constructed wetlands using *Typha angustifolia* in combination with catalytic ozonation on Fe-zeolite A,” *International Journal of Phytoremediation*, vol. 23, pp. 809–817, 2021.
- [19] N. Tahir, M. Zahid, H. N. Bhatti et al., “Silver-doped ternary compounds for wastewater remediation,” in *Silver Nanomaterials for Agri-Food Applications*, pp. 623–653, Elsevier, 2021.
- [20] M. Madkour, Y. Abdelmonem, U. Y. Qazi, R. Javaid, and S. Vadivel, “Efficient Cr(vi) photoreduction under natural solar irradiation using a novel step-scheme ZnS/SnIn₄S₈ nano-heterostructured photocatalysts,” *RSC Advances*, vol. 11, no. 47, pp. 29433–29440, 2021.
- [21] N. Fatima, U. Y. Qazi, A. Mansha et al., “Recent developments for antimicrobial applications of graphene-based polymeric composites: a review,” *Journal of Industrial and Engineering Chemistry*, vol. 100, pp. 40–58, 2021.
- [22] U. Y. Qazi, R. Javaid, M. Zahid, N. Tahir, A. Afzal, and X. M. Lin, “Bimetallic NiCo–NiCoO₂ nano-heterostructures embedded on copper foam as a self-supported bifunctional electrode for water oxidation and hydrogen production in alkaline media,” *International Journal of Hydrogen Energy*, vol. 46, no. 36, pp. 18936–18948, 2021.
- [23] N. M. Mahmoodi and M. H. Saffar-Dastgerdi, “Zeolite nanoparticle as a superior adsorbent with high capacity: synthesis, surface modification and pollutant adsorption ability from wastewater,” *Microchemical Journal*, vol. 145, pp. 74–83, 2019.
- [24] Y. Xu, Q. Wang, B. A. Yoza et al., “Catalytic ozonation of recalcitrant organic chemicals in water using vanadium oxides loaded ZSM-5 zeolites,” *Frontiers in Chemistry*, vol. 7, p. 384, 2019.
- [25] H. Einaga and S. Futamura, “Catalytic oxidation of benzene with ozone over Mn ion-exchanged zeolites,” *Catalysis Communications*, vol. 8, no. 3, pp. 557–560, 2007.
- [26] J. A. Medrano, A. Garofalo, L. Donato et al., “CO selective oxidation using catalytic zeolite membranes,” *Chemical Engineering Journal*, vol. 351, pp. 40–47, 2018.
- [27] H. Valdés, V. J. Farfán, J. A. Manoli, and C. A. Zaror, “Catalytic ozone aqueous decomposition promoted by natural zeolite and volcanic sand,” *Journal of Hazardous Materials*, vol. 165, no. 1-3, pp. 915–922, 2009.
- [28] A. Ikhlq, S. Waheed, K. S. Joya, and M. Kazmi, “Catalytic ozonation of paracetamol on zeolite a: non-radical mechanism,” *Catalysis Communications*, vol. 112, pp. 15–20, 2018.
- [29] C. W. Kwong, C. Y. H. Chao, K. S. Hui, and M. P. Wan, “Catalytic ozonation of toluene using zeolite and MCM-41 materials,” *Environmental Science & Technology*, vol. 42, no. 22, pp. 8504–8509, 2008.
- [30] Y. Kitada, H. Kawahata, A. Suzuki, and T. Oomori, “Catalytic activity and stability of Y zeolite for phenol degradation in the presence of ozone,” *Applied Catalysis B: Environmental*, vol. 82, no. 3-4, pp. 163–168, 2008.
- [31] N. A. S. Amin, J. Akhtar, and H. K. Rai, “Catalytic ozonation of aqueous phenol over metal-loaded HZSM-5,” *Water Science and Technology*, vol. 63, no. 8, pp. 1651–1656, 2011.
- [32] C. Chen, X. Yan, B. A. Yoza et al., “Efficiencies and mechanisms of ZSM5 zeolites loaded with cerium, iron, or manganese oxides for catalytic ozonation of nitrobenzene in water,” *Science of the Total Environment*, vol. 612, pp. 1424–1432, 2018.
- [33] A. Ikhlq and B. Kasprzyk-Hordern, “Catalytic ozonation of chlorinated VOCs on ZSM-5 zeolites and alumina: formation of chlorides,” *Applied Catalysis B: Environmental*, vol. 200, pp. 274–282, 2017.

- [34] K. González-Labrada, R. Richard, C. Andriantsiferana, H. Valdés, U. J. Jáuregui-Haza, and M. H. Manero, "Enhancement of ciprofloxacin degradation in aqueous system by heterogeneous catalytic ozonation," *Environmental Science and Pollution Research*, vol. 27, no. 2, pp. 1246–1255, 2020.
- [35] A. Ikhlaq, D. R. Brown, and B. Kasprzyk-Hordern, "Mechanisms of catalytic ozonation: an investigation into superoxide ion radical and hydrogen peroxide formation during catalytic ozonation on alumina and zeolites in water," *Applied Catalysis B: Environmental*, vol. 129, pp. 437–449, 2013.
- [36] A. J. Watkinson, E. J. Murby, D. W. Kolpin, and S. D. Costanzo, "The occurrence of antibiotics in an urban watershed: from wastewater to drinking water," *Science of the Total Environment*, vol. 407, no. 8, pp. 2711–2723, 2009.
- [37] W. Li, Y. Shi, L. Gao, J. Liu, and Y. Cai, "Occurrence of antibiotics in water, sediments, aquatic plants, and animals from Baiyangdian Lake in North China," *Chemosphere*, vol. 89, no. 11, pp. 1307–1315, 2012.
- [38] J. Xu, Y. Xu, H. Wang et al., "Occurrence of antibiotics and antibiotic resistance genes in a sewage treatment plant and its effluent-receiving river," *Chemosphere*, vol. 119, pp. 1379–1385, 2015.
- [39] R. Javaid and U. Y. Qazi, "Catalytic oxidation process for the degradation of synthetic dyes: an overview," *International Journal of Environmental Research and Public Health*, vol. 16, no. 11, article 2066, 2019.
- [40] L. Hu, G. X. Hao, H. D. Luo et al., "Bifunctional 2D cd(II)-based metal-organic framework as efficient heterogeneous catalyst for the formation of C-C bond," *Crystal Growth & Design*, vol. 18, no. 5, pp. 2883–2889, 2018.
- [41] A. Zeb, S. Sahar, U. Y. Qazi et al., "Intrinsic peroxidase-like activity and enhanced photo-Fenton reactivity of iron-substituted polyoxometallate nanostructures," *Dalton Transactions*, vol. 47, no. 21, pp. 7344–7352, 2018.
- [42] H. H. Zou, C. Z. Yuan, H. Y. Zou et al., "Bimetallic phosphide hollow nanocubes derived from a prussian-blue-analog used as high-performance catalysts for the oxygen evolution reaction," *Science and Technology*, vol. 7, no. 7, pp. 1549–1555, 2017.
- [43] A. Ikhlaq, M. Anis, F. Javed et al., "Catalytic ozonation for the treatment of municipal wastewater by iron loaded zeolite A," *Desalin Water Treat*, vol. 152, pp. 108–115, 2019.
- [44] Y. Flores, R. Flores, and A. A. Gallegos, "Heterogeneous catalysis in the Fenton-type system reactive black 5/H₂O₂," *Journal of Molecular Catalysis A: Chemical*, vol. 281, no. 1-2, pp. 184–191, 2008.
- [45] F. Adam, T. S. Chew, and J. Andas, "A simple template-free sol-gel synthesis of spherical nanosilica from agricultural biomass," *Journal of Sol-Gel Science and Technology*, vol. 59, no. 3, pp. 580–583, 2011.
- [46] A. D. Eaton, M. A. H. Franson, L. S. Clesceri, E. W. Rice, and A. E. Greenberg, *Standard methods for the examination of water & wastewater*, American Public Health Association (APHA), Washington, DC, USA, 2005.
- [47] M. Tekbaş, H. C. Yatmaz, and N. Bektaş, "Heterogeneous photo-Fenton oxidation of reactive azo dye solutions using iron exchanged zeolite as a catalyst," *Microporous and Mesoporous Materials*, vol. 115, no. 3, pp. 594–602, 2008.
- [48] J. P. Reymond and F. Kolenda, "Estimation of the point of zero charge of simple and mixed oxides by mass titration," in *Powder Technol.*, pp. 30–36, Elsevier Sequoia SA, 1999.
- [49] D. Gümüş and F. Akbal, "A comparative study of ozonation, iron coated zeolite catalyzed ozonation and granular activated carbon catalyzed ozonation of humic acid," *Chemosphere*, vol. 174, pp. 218–231, 2017.
- [50] A. Ikhlaq, D. R. Brown, and B. Kasprzyk-Hordern, "Catalytic ozonation for the removal of organic contaminants in water on alumina," *Applied Catalysis B: Environmental*, vol. 165, pp. 408–418, 2015.
- [51] S. Gomez, L. Lericci, C. Saux et al., "Fe/ZSM-11 as a novel and efficient photocatalyst to degrade Dichlorvos on water solutions," *Applied Catalysis B: Environmental*, vol. 202, pp. 580–586, 2017.
- [52] A. Latifoglu and M. D. Gurol, "The effect of humic acids on nitrobenzene oxidation by ozonation and O₃/UV processes," *Water Research*, vol. 37, no. 8, pp. 1879–1889, 2003.
- [53] J. Choina, H. Kosslick, C. Fischer, G. U. Flechsig, L. Frunza, and A. Schulz, "Photocatalytic decomposition of pharmaceutical ibuprofen pollutions in water over titania catalyst," *Applied Catalysis B: Environmental*, vol. 129, pp. 589–598, 2013.
- [54] D. Shan, S. Deng, C. Jiang et al., "Hydrophilic and strengthened 3D reduced graphene oxide/nano-Fe₃O₄ hybrid hydrogel for enhanced adsorption and catalytic oxidation of typical pharmaceuticals," *Nano*, vol. 5, no. 7, pp. 1650–1660, 2018.
- [55] Y. Sun, H. Li, G. Li, B. Gao, Q. Yue, and X. Li, "Characterization and ciprofloxacin adsorption properties of activated carbons prepared from biomass wastes by H₃PO₄ activation," *Bioresource Technology*, vol. 217, pp. 239–244, 2016.
- [56] N. Kishimoto, Y. Yasuda, H. Mizutani, and Y. Ono, "Applicability of ozonation combined with electrolysis to 1,4-Dioxane removal from wastewater containing radical scavengers," *Ozone Science and Engineering*, vol. 29, no. 1, pp. 13–22, 2007.
- [57] A. Ikhlaq, D. R. Brown, and B. Kasprzyk-Hordern, "Mechanisms of catalytic ozonation on alumina and zeolites in water: formation of hydroxyl radicals," *Applied Catalysis B: Environmental*, vol. 123-124, pp. 94–106, 2012.
- [58] R. Gonzalez-Olmos, U. Roland, H. Toufar, F. D. Kopinke, and A. Georgi, "Fe-zeolites as catalysts for chemical oxidation of MTBE in water with H₂O₂," *Applied Catalysis B: Environmental*, vol. 89, no. 3-4, pp. 356–364, 2009.